Production Systems and Information Engineering
Volume 5 (2009), pp. 167-175.

LOOK UP TABLE EDITOR FOR SMALL ANIMAL PET INSTRUMENT

Ákos Szlávecz
Budapest University of Technology and Economics, Hungary
Department of Control Engineering and Information Technology
szlavecz@iit.bme.hu

Gábor Hesz
Budapest University of Technology and Economics, Hungary
Department of Control Engineering and Information Technology
hesz@iit.bme.hu

Péter Major
Mediso Ltd., Hungary
major.peter@mediso.hu

Balázs Benyó
Budapest University of Technology and Economics, Hungary
Department of Control Engineering and Information Technology
bbenyo@iit.bme.hu

[Received April 2009 and accepted June 2009]

Abstract. Small animal PET is a widely used instrument for functional examinations in pharmaceutical industry research; its spatial resolution has reached the physically possible limit by now. One important issue of the imaging process is to determine the position of γ photons impacting the surface of the detectors, and to filter them based on their energy. In this paper we introduce the methods developed to complete these tasks for the small animal PET instrument of Mediso Ltd. All the introduced methods have been implemented in an application called LUT-QT. The efficiency of the methods has been evaluated in real experiments.

Keywords: Positron Emission Tomography (PET), position discrimination, energy discrimination

1. Introduction

Positron Emission Tomography (PET) [1], [2] has become a fundamental instrument of functional examinations over the past two decades. Even though its spatial resolution fails to keep level with anatomical examinations, e.g.

X-ray tomography (abbreviated CT), PET allows monitoring the track of a selected molecule, traced with radioactive isotopes, within the organism examined, which may lead to conclusions about the functioning or eventual abnormalities of certain organs. Clinical (i.e. human) PET instruments nowadays operate with a spatial resolution of about 3-5 mm considering the rational cost limits as the consequence of the large size, whereas a spatial resolution of pre-clinical (or small animal) PET instruments has reached the theoretic limit of 1-2 mm attainable with positron annihilation. That quality is necessary because in pharmaceutical industry research the operation of the internal organs of experimental mice needs to be monitored. Therefore, in addition to a very good spatial resolution, small animal instruments have to meet another important requirement: because of the statistical nature of impact mechanism tests of drugs a great number of mice must be examined under identical circumstances to obtain a reliable result, so the examination should be very fast (a couple of minutes). In order to understand the problems of data processing we have addressed, let us review the imaging process in brief.

2. Main steps of PET imaging process

Injecting some positron (β^+) emitting marker into the investigated organism, a positron is produced through decay of the marker. The positron hits an electron within the positron range [3] and both get annihilated. In a medium with a density close to that of water, it is about 1 mm. In consequence of conservation of impulse and energy, two γ photons with 511 keV energy are produced leaving in approximately 180^o, neglecting the non-collinearity effect [4] as can be seen in Figure 1. If we can detect these photons, we can determine the line (line of response, LOR) along which the annihilation has happened. Having the data of several million LORs, we can estimate the density of the marker in each small space unit (the so-called voxel) because the number of lines (LORs) going through a space unit is proportional to the number of local decays. The condition of coincidence ensures that the detected photons originate from the same event: the data gathering device keeps only events arriving within a certain small time window (typically 5ns), otherwise we would get false LORs connecting the positions of two impacts from two independent annihilations. This means that we need to know exactly the LORs and therefore the impact positions of the γ photons in order to have a proper spatial resolution. Generally, detecting photons with such high energy is feasible with scintillation crystal, [5] a material which absorbes the incoming photons with high probability, producing a visible light flash. If we put scintillation crystal needles in a matrix made of reflecting material arranged as septa, the subsequent flash will remain localised in two directions, which helps the determination of the impact position. Therefore the task is to determine the flashing crystal needle for each event. One of the issues we have addressed was that localisation based on the detector signals.

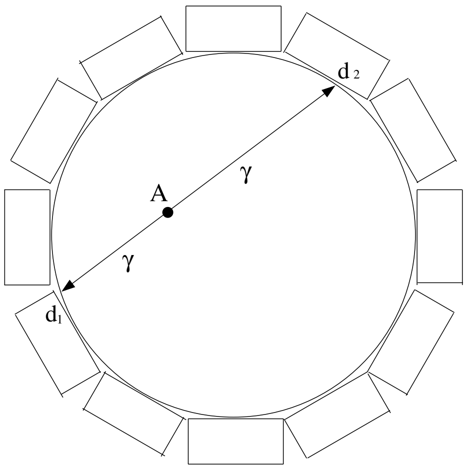

Figure 1. Antiparallel 511 keV γ photons produced from positron annihilation at point 'A' and the line (line of response, LOR) connecting the positions of detection (d_1, d_2)

3. Determining the position of detected γ photons

In the case of our device, a Hamamatsu H-9500 position sensitive detector with 16x16 sensors (anodes) converts the flashes of the crystal matrix made of 35x35 pcs, 1.27 mm x 1.27 mm LYSO needles, and the created electrical signals can be used to determine the needle that produced the flash. The setup of the detector module is basically the same as described in [6] although the needles area thinner and the electronics has been modified. In the course of the fast examinations mentioned in the introduction we must handle several hundred thousand events per second, hence the digitalization and processing of all the 256 detector signals would be impossible at this data processing speed. Therefore the usual process is to add up the anode signals with a resistor network, wherein the anode currents are weighted with resistors in such a way that the difference of the resultant currents in the corners of the network is more or less proportional to the coordinate of the anode. This method produces a distorted, but two-dimensional image called Anger image [7]. Thus the task is to prepare a table (Look Up Table, abbreviated LUT) for each detector, which assigns a crystal needle index to arbitrary detector signals (x and y Anger-coordinates). In order to determine a certain detector signal position map, we start from the image of the homogenously irradiated detector, the so-called Flood-field image, which is actually the impact number as the function of the two-dimensional (2D) position. Each crystal needle has its own light cloud in the Flood-field image, we need to find the centre of the light clouds of the crystal needles and label them with the proper needle indices. As soon as we have found the centre of the light cloud of every crystal needle, we should be able to determine in case of any (x,y) points the light cloud of which needle is the closest to it, and we should assign it to that needle. Because of the speed of data gathering it is worth calculating a two-dimensional map preliminarily, i.e. we determine the closest needle to each point of the image space covering the certain distorted quadratic lattice (the centers of the needle clouds) sized 35x35. In other words, we store the ranges of points closest to the centres (Wigner-Seitz cell or Voronoi-cell) in a matrix, in which a matrix cell, assigned to an incoming event's discrete (x,y) coordinate as an index, contains the proper needle index. As a consequence, based on the coordinate (x,y) produced as a result of measurement, if we have this matrix we immediately know the index of the flashing needle without any further calculation.

During the search for the light clouds of the needles we must first of all filter the image because of the Poisson statistics of the light produced in scintillation and the noise of the electronic signals. We have selected the matrix of the convolution filter used to have isotropic smoothing in the x-y plane, since the light clouds have a circular shape. In case of the 5x5 unit matrix for example, the characteristic distance of smoothing is $\sqrt{2}$ times larger in the direction of the diagonal, so we have chosen such weights as elements of the convolution matrix that a circle with r=2.5 units would cover from a given pixel of the quadratic lattice of 5x5 (a.k.a. disk filter). Then an automatic algorithm finds the valleys between the clouds and then finds the centre of the light clouds in the areas defined by the intersections of the valleys. It seemed to be uncertain to search for a maximum based on the derivative because of the accidental nature of impact numbers and the noises, plus exaggerated smoothing will shift culminations, thus we are searching for the centre of gravity in a given area, where the 'weight' is the impact number. The process is iterative; it defines an environment around the initial point in a given iteration, determines its centre of gravity, defines its environment, etc.

Finding every light cloud automatically is especially difficult in case of the crystal needles at the edges of the detector because of the natural distortions of the Anger image; the spots get closer to each other and they run into one another, furthermore, the signal to noise ratio is the worst in that area. On the other hand, different optical faults are also possible, e.g. poor optical connection between the detector and the crystal matrix, the lack of optical grease leads to intensity decrease, or an air bubble in the optical grease produces lens impact. Sometimes a deficient crystal needle is misplaced or it has lower intensity or disappears completely. To ensure a good performance, we have decided to integrate the options of check-up and manual correction into LUT-QT after the automatic algorithm. (See Figure 2.)

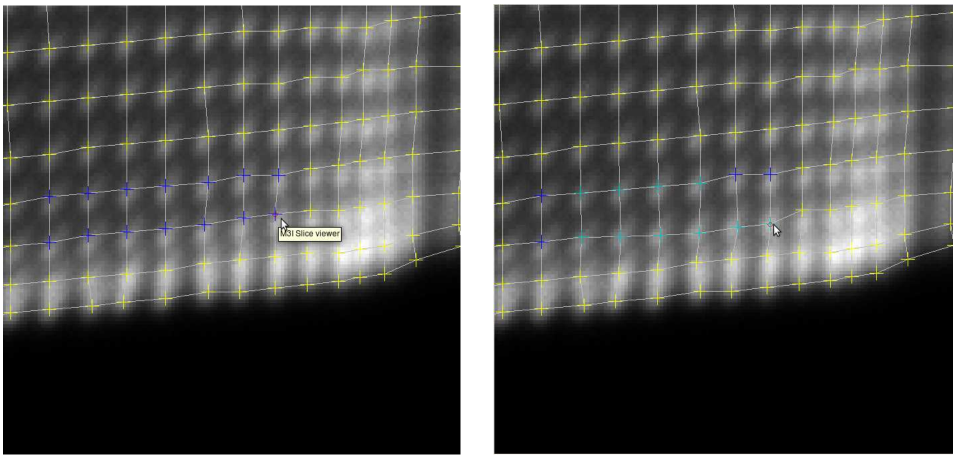

a., **b.,**

Figure 2. Figure **a.,** shows part of a Flood-field image with mistakenly detected light clouds (crosses mark the spots detected by LUT-QT). Figure **b.,** shows image during manual correcting.

Projecting the measured Flood-field image and the centres of the crystal needles we assume to have found on the graphical user surface of LUT-QT, the grid of the latter is modifiable according to either points or range. In order to enable modification of ranges, we have searched for a 2D transformation (distortion), which can act as displacement, enlargement, rotation, shearing or any required combination of those. It has 8 parameters and can transform a rectangle not only into a parallelogram but into a general trapezoid as well. The input data are the displacements of the four corners of the range to be distorted (4 2D vectors). We get the displacements of the interior points of the initial quadrilateral by weighting the displacements of the corners, just like in case of the coordinates of the point of division. That transformation corresponds to the characteristics listed. The range to be modified and the new corners are displayed in Figure 3 with an interior point P of the range. Using the notation in Figure 3, displacement of point P in direction x is:

$$\mathbf{e}_P(x) = \left(\frac{d_f}{c_f+d_f}\cdot\frac{b_b}{a_b+b_b}\cdot\mathbf{e}_1(x)+\frac{c_f}{c_f+d_f}\cdot\frac{b_j}{a_j+b_j}\cdot\mathbf{e}_2(x)+ + \frac{d_a}{c_a+d_a}\cdot\frac{a_b}{a_b+b_b}\cdot\mathbf{e}_3(x)+\frac{c_a}{c_a+d_a}\cdot\frac{a_j}{a_j+b_j}\cdot\mathbf{e}_4(x)\right) \quad (3.1)$$

and similarly the y component of the displacement of point P is:

$$\mathbf{e}_P(y) = \left(\frac{d_f}{c_f+d_f}\cdot\frac{b_b}{a_b+b_b}\cdot\mathbf{e}_1(y)+\frac{c_f}{c_f+d_f}\cdot\frac{b_j}{a_j+b_j}\cdot\mathbf{e}_2(y)+ + \frac{d_a}{c_a+d_a}\cdot\frac{a_b}{a_b+b_b}\cdot\mathbf{e}_3(y)+\frac{c_a}{c_a+d_a}\cdot\frac{a_j}{a_j+b_j}\cdot\mathbf{e}_4(y)\right) \quad (3.2)$$

After the eventual manual modification we can reiterate the centre of gravity search around the new corners. Figure 5/a shows the distorted Anger image and the light spot centres determined with LUT-QT of a detector with several faults.

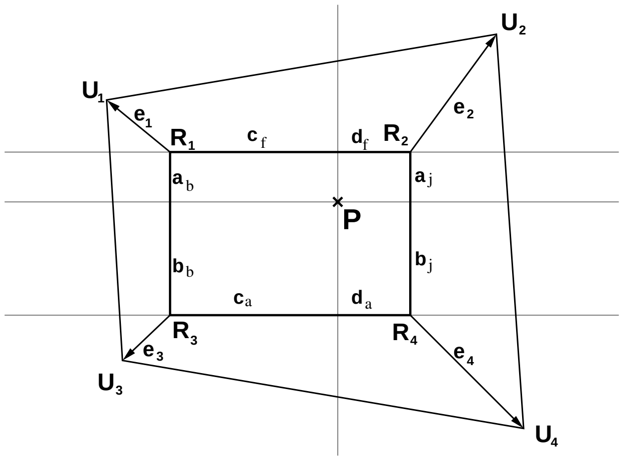

Figure 3. 'Old' (R_1,R_2,R_3,R_4) corner points, their new (U_1,U_2,U_3,U_4) positions, (e_1,e_2,e_3,e_4) displacement vectors and point P of the selected range

4. Energy of the detected γ photons

As a consequence of detection with scintillation crystal, certain signals have to be filtered, because one part of the γ photons participates in scattering where only a part of their energy is absorbed and the direction of their speed changes, sometimes they can induce further scintillations in other positions, making their localisation theoretically impossible. However, that makes local correction of the energy of events necessary, as the sensitivity of the detectors is not homogenous. The magnitude of the detector signals is proportional to the transmitted energy of the impacted γ photon. As soon as we have resolved the localisation of the detected γ photons, there is nothing to prevent us from preparing the incoming event's detector signal histogram for each crystal needle separately. That will give us the energy-histogram, if we manage to find the proportion coefficient (as the function of position) between detector signal and energy. Thus creating a local energy scale adapted to the inhomogeneous amplification of the detector will become possible, as well as consequent local energy filtering.

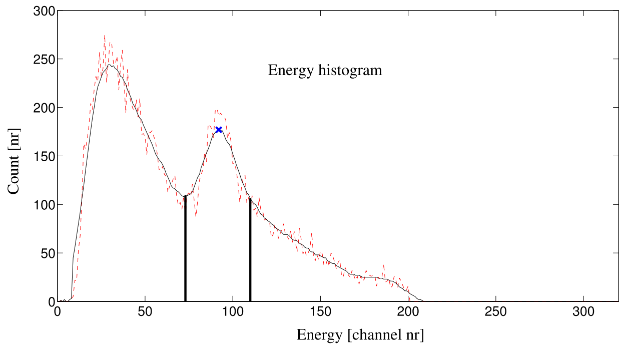

Figure 4. Energy histogram of events detected by a selected (No. 137) crystal needle. The raw curve is shown by a broken line, the curve smoothed with convolution filter by a continuous line; columns show the energy gates and the sign $\times$ shows the photopeak.

Since we allocate the events collected during measurement among 1225 crystal needles, the energy spectrum statistics for a single needle is not very good; they are rather noisy. However, the task is fairly simple, as we search for the right hand peak in the histogram smoothed with the convolution filter, which is actually the photopeak. In case of a properly selected threshold, where the two intervals of the events with impact number higher than the threshold would merge, the limits of the right hand interval will be the events with appropriate energy. Local scaling and filtering can be performed based on the fact that the position of the peak corresponds to 511 keV on the energy scale, and the noise level of the Anger image will subsequently have a significant decrease. Figure 4 shows the energy spectrum of a selected crystal needle, the photopeak and local energy gates.

5. Results

Figure 5/b shows a reconstructed image made by a small animal PET instrument using energy filter and position maps prepared with LUT-QT. In order to examine spatial resolution we have positioned a plastic cylinder (called Derenzo phantom) with holes of different diameters filled with isotopes in the scope of the device, the diameters of the cylinders being 1.6-2.1 mm. Since the images of each cylinder are shown isolated, spatial resolution is smaller than 1.6 mm.

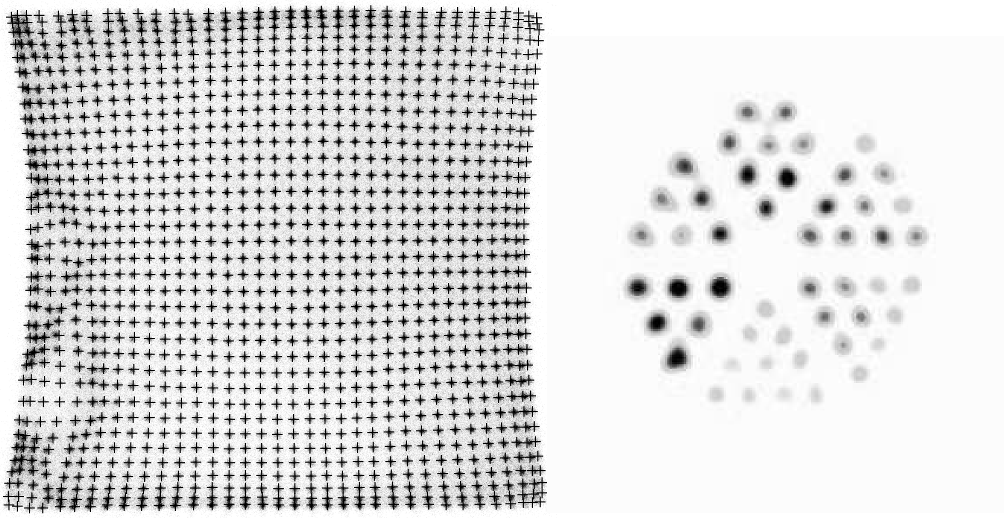

a., **b.,**

Figure 5. Figure **a.,** shows the Flood-field image of a faulty detector module, crosses mark the spots detected by LUT-QT. Figure **b.,** shows the reconstructed image of a Derenzo phantom positioned in the field of view of the small animal PET instrument (activity: ≈ 4 MBq FDG, acquisition time: 30 minutes).

6. Summary

Problem specific methods have been developed to create detector signal position maps used in Mediso's small animal PET instrument. The methods have been implemented in the LUT-QT application. The detector signal – crystal needle index matrix – created from Flood-field images of the single detectors, determining the centres of light clouds on the adequately filtered images makes quick and accurate determination of the position of incoming γ photons possible. The operation of the code has been successfully tested on real measurement data. Our further aim is to reduce the computation time of the LUT-QT application by optimizing the code and to stabilize the automatic search for light spots, and we would like to develop the possibility of the automatic correction of eventual slow and continuous changes (i.e. because of the outside temperature) in the amplification of the detector signals.

7. Acknowledgements

This work was supported by Mediso Ltd., by the National Office for Research and Technology (NKTH) Grants No. NKFP-A1-2006-0017 (PETCT) and TECH-08-A2-TeraTomo, and by the Hungarian National Research Found (OTKA) Grant No. T69055. We express our thanks for the help and the inspiring and forward-looking debates with our colleagues, László Árvai, László Balkay, Tamás Bükki, Balázs Domonkos, Gábor Jakab, Gábor Németh, Gergely Németh, Gergely Patay and Sándor Török.

REFERENCES

[1] Muehllehner, G. and Karp, J. S.: Positron Emission Tomography. *Phys. Med. Biol.*, **51**, (2006), 117–137.

[2] Lewellen, T. K.: Recent developments in PET detector technology. *Phys. Med. Biol.*, **53**, (2008), 287–317.

[3] Levin, C. S. and Hoffman, E. J.: Calculation of positron range and its effect on the fundamental limit of positron emission tomography system spatial resolution. *Phys. Med. Biol.*, **44**, (1999), 781–799.

[4] Shibuya, K., Yoshida, E., Nishikido, F., Suzuki, T., Inadama, N., Yamaya, T., and Murayama, H.: A healthy volunteer FDG-PET study on annihilation radiation non-collinearity. In *IEEE Nuclear Science Symposium Conference Record*, vol. 3, 2006, pp. 1889–1892.

[5] Doshi, N. K., Williams, C. W., Schmand, M., Andreaco, M., Aykac, M., Loope, M. D., Eniksson, L. A., Melcher, C. L., and Nutt, R.: Comparison of typical scintillators for PET. In *IEEE Nuclear Science Symposium Conference Record*, vol. 3, 2002, pp. 1420–1423.

[6] Imrek, J., Hegyesi, G., Kalinka, G., Molnar, J., Novak, D., Valastyan, I., Vegh, J., Balkay, L., Emri, M., Kis, S., Tron, L., Bükki, T., Szabo, Z., and Kerek, A.: Development of an improved detector module for miniPET-II. In *IEEE Nuclear Science Symposium Conference Record*, vol. 5, 2006, pp. 3037–3040.

[7] Anger, H. O.: Survey of radioisotope cameras. *J. Nucl. Med.*, **5**, (1966), 311–334.